Hyperfine structure in the HD molecule

Jacek Komasa and Mariusz Puchalski
Faculty of Chemistry, Adam Mickiewicz University, Uniwersytetu Poznańskiego 8, 61-614 Poznań, Poland

Krzysztof Pachucki
Faculty of Physics, University of Warsaw, Pasteura 5, 02-093 Warsaw, Poland

(Received 6 May 2020; accepted 2 July 2020; published 23 July 2020)

We investigate interactions between the proton spin, the deuteron spin, and the orbital angular momentum in the electronic ground state of the HD molecule. These interactions lead to hyperfine splittings of molecular energy levels. Our numerical results for the first rotational level agree well with the currently most accurate measurement performed by Ramsey *et al.* [Phys. Rev. **112**, 1929 (1958)] in the 1950s. Knowledge of the hyperfine structure of other levels is necessary for the accurate determination of rovibrational transition energies in spectroscopic measurements. We present theoretical predictions and share the numerical code used to perform numerical calculations. This paper sets the groundwork for high-precision spectroscopic tests of hyperfine interactions in molecular systems. In particular we determine the value of the deuteron quadrupole moment $Q = 0.2856(2)$ fm^2 and give an outlook for improving its accuracy by three orders of magnitude.

DOI: 10.1103/PhysRevA.102.012814

I. INTRODUCTION

Current theoretical predictions for the hyperfine structure (hfs) in simple molecules are far less accurate than the experimental values obtained in original microwave measurements by Ramsey and coworkers [1,2] half a century ago. For HD these measurements were performed, regrettably, only for the lowest rotational level. On the other hand, theoretically predicted hyperfine structure (hfs) of many other molecular levels is necessary for a contemporary determination of transition frequencies, due to the complexity of the line shape. For instance, several recent measurements [3–5] of a specific transition frequency in HD significantly disagree with each other, presumably because of a different line-shape modeling that has been employed. Therefore, the knowledge of the hyperfine splitting and corresponding individual transition rates is of crucial importance in a correct interpretation of precision molecular spectroscopy.

The first step in this direction is the recent work of Dupré [6], which presents results for low-lying vibrational levels with the rotational number $J = 1$, however without any uncertainties. In this paper we present a systematic derivation and numerical calculation of leading hyperfine interactions for all molecular levels in the HD molecule, including individual hfs transition rates between them, within the Born-Oppenheimer (BO) approximation. Due to this approximation our results will have about 10^{-3} relative accuracy, which nevertheless is sufficient for the current experimental precision of rovibrational transitions. Moreover, we present hyperfine splittings for an arbitrary rovibrational level of HD in terms of a freely available computer code [7]. As well as application in molecular spectroscopy, our results could also be useful in precision tests of hyperfine interactions in the HD molecule, provided the theory for relativistic and quantum electrodynamic corrections is developed.

Considering theory for the leading molecular hyperfine structure [8], there are three angular momenta in the ground electronic state of the HD molecule: the proton spin $\vec{I}_p$, that of the deuteron $\vec{I}_d$, and the rotational angular momentum $\vec{J}$. All of them interact with each other, and using the Ramsey notation (e.g., Ref. [9]) the effective Hamiltonian describing these interactions reads

$$H_{\rm hfs} = -c_p\,\vec{I}_p\cdot\vec{J} - c_d\,\vec{I}_d\cdot\vec{J} + \frac{5\,d_1}{(2J-1)(2J+3)} \times\left[\frac{3}{2}\,(\vec{I}_p\cdot\vec{J})\,(\vec{I}_d\cdot\vec{J}) + \frac{3}{2}(\vec{I}_d\cdot\vec{J})(\vec{I}_p\cdot\vec{J}) - (\vec{I}_p\cdot\vec{I}_d)\,\vec{J}^{\,2}\right] + \frac{5d_2}{(2J-1)(2J+3)}\left[3(\vec{I}_d\cdot\vec{J})^2+\frac{3}{2}(\vec{I}_d\cdot\vec{J})-\vec{I}_d^{\,2}\,\vec{J}^{\,2}\right]. \tag{1}$$

One observes the lack of a separate $\vec{I}_p\cdot\vec{I}_d$ coupling. The direct scalar nuclear spin-spin interaction vanishes, while the electron-mediated nuclear spin-spin interaction is of higher order in the fine-structure constant α. Namely, it is α^2 times smaller than the above tensor interactions and therefore is neglected here as are all the other α^2 corrections.

The above coefficients c_p, c_d, d_1, and d_2 are related, respectively, to the interactions between the proton spin and molecular rotation, the deuteron spin and rotation, the proton and deuteron spins, and the electric quadrupole moment of the deuteron with the electric-field gradient. All of these constants depend on the molecular level, identified by the vibrational v and the rotational J quantum numbers.

In the following sections, we present a short derivation of all the constants, followed by their numerical calculation as functions of the internuclear distance R. Their values for a particular molecular state are obtained by averaging with the

nuclear wave function $\chi_{v,J}$:

$$H_{\rm hfs}(v,J) = \langle v,J|H_{\rm hfs}(R)|v,J\rangle. \tag{2}$$

This is an approximate treatment that relies on the BO approximation, but it is a good starting point for future more accurate nonadiabatic calculations. Ramsey, in his monograph on molecular beams [10], presented a basic theory of nuclear and rotational magnetic moment coupling. Here, we present a concise and rigorous derivation of all molecular hfs interactions, which can also be a basis for the derivation of relativistic as well as QED corrections.

II. NUCLEAR SPIN-ROTATION CONSTANTS c_p AND c_d

The following derivation of the spin-rotation constant is based on our former work [11], from which we adopt the notation. Let us consider a Hamiltonian for a particle with charge e, mass M, spin I, and a gyromagnetic factor g, interacting with the electromagnetic field ($\hbar = c = 1$):

$$H = \frac{\vec{\pi}^2}{2M} + eA^0 - \frac{e\,g}{2M}\,\vec{I}\cdot\vec{B} - \frac{e\,(g-1)}{4M^2}\,\vec{I}\cdot(\vec{E}\times\vec{\pi} - \vec{\pi}\times\vec{E}), \tag{3}$$

where $\vec{\pi} = \vec{p} - e\vec{A}$. If this particle is the proton or deuteron, then e coincides with the elementary charge. The gyromagnetic factors

$$g_p = \frac{\mu_p}{\mu_N\, I_p} = 5.585\,695\ldots, \tag{4}$$

$$g_d = \frac{\mu_d}{\mu_N\, I_d}\,\frac{m_d}{m_p} = 1.714\,025\ldots \tag{5}$$

are related to the magnetic moment of the proton $\mu_p = 2.792\,847\,344\,63(82)\,\mu_N$ and the deuteron $\mu_d = 0.857\,438\,2338(22)\,\mu_N$, respectively [12]. The g factor is a dimensionless quantity which is more convenient to use in formulas than the magnetic moment. If the electromagnetic field comes from the other nucleus or from the electron, it is of the form

$$\vec{E} = -\frac{e}{4\pi}\,\frac{\vec{r}}{r^3}, \tag{6}$$

$$A^i = \frac{e}{4\pi}\left[\frac{1}{2r}\left(\delta^{ij} + \frac{r^i\,r^j}{r^2}\right)p^j - \frac{g}{2M}\,\vec{I}\times\frac{\vec{r}}{r^3}\right], \tag{7}$$

where i, j are Cartesian indices, and, in the case of an electron $g = 2$, M becomes the electron mass m. Inserting the above formulas into Eq. (3) one obtains the general spin-orbit Hamiltonian

$$\delta H = \sum_{\alpha,\beta}\frac{e_\alpha\,e_\beta}{4\pi}\,\frac{1}{2r_{\alpha\beta}^3}\left[\frac{g_\alpha}{m_\alpha\,m_\beta}\,\vec{I}_\alpha\cdot\vec{r}_{\alpha\beta}\times\vec{p}_\beta - \frac{(g_\alpha-1)}{m_\alpha^2}\,\vec{I}_\alpha\cdot\vec{r}_{\alpha\beta}\times\vec{p}_\alpha\right], \tag{8}$$

where the indices α and β go over both electrons and nuclei. In particular, the coupling of the nuclear spin $\vec{I} = \vec{I}_A$ to the molecular rotation is

$$\delta_A H = \sum_b \frac{e_A\,e}{4\pi}\,\frac{\vec{I}}{2r_{Ab}^3}\left[\frac{g_A}{m_A\,m}\,\vec{r}_{Ab}\times\vec{p}_b - \frac{(g_A-1)}{m_A^2}\,\vec{r}_{Ab}\times\vec{p}_A\right] + \frac{e_A\,e_B}{4\pi}\,\frac{\vec{I}}{2r_{AB}^3}\cdot\left[\frac{g_A}{m_A\,m_B}\,\vec{r}_{AB}\times\vec{p}_B - \frac{(g_A-1)}{m_A^2}\,\vec{r}_{AB}\times\vec{p}_A\right]. \tag{9}$$

For convenience, following Ref. [11], we chose the reference frame centered at the considered nucleus A and introduced the notation $\vec{R} = \vec{r}_{AB}$, $\vec{P} = -\imath\,\vec{\nabla}_R$, and $\vec{x}_b = \vec{r}_{bA} = \vec{r}_b - \vec{r}_A$. For the Σ_g^+ electronic state considered here, $\delta_A H$ takes the form

$$\delta_A H = \vec{Q}_1\cdot\vec{I} + \vec{Q}_2\times\vec{P}\cdot\vec{I}, \tag{10}$$

$$\vec{Q}_1 = -\sum_b\frac{e_A\,e}{4\pi}\,\frac{g_A}{2m\,m_A}\,\frac{\vec{x}_b\times\vec{p}_b}{x_b^3}, \tag{11}$$

$$\vec{Q}_2 = -\sum_b\frac{e_A\,e}{4\pi}\,\frac{1}{2m_A^2}\,\frac{\vec{x}_b}{x_b^3} - \frac{e_A\,e_B}{4\pi}\,\frac{1}{2m_A}\left[\frac{g_A}{m_B} + \frac{(g_A-1)}{m_A}\right]\frac{\vec{R}}{R^3}, \tag{12}$$

where we neglected terms of the higher order in the electron-nucleus mass ratio. We make use of BO approximation, and the total wave function ψ is represented as a product

$$\psi_{v,J,M} = \phi_{\rm el}(\vec{x}_a)\,\chi_{v,J}(R)\,Y_{J,M}(\vec{n}) \tag{13}$$

of the electronic wave function $\phi_{\rm el}(\vec{x}_a)$, the nuclear one $\chi_{v,J}(R)$, and the spherical harmonic $Y_{J,M}(\vec{n})$, where $\vec{n} = \vec{R}/R$. The electronic wave function $\phi_{\rm el}$ for the ground Σ^+ state is a scalar function, and thus depends only on interparticle distances.

The expectation value of $\langle\phi_{\rm el}|\vec{Q}_1|\phi_{\rm el}\rangle$ vanishes and the $\vec{Q}_1$ operator contributes only through the nonadiabatic matrix element [11]

$$\langle\vec{Q}\rangle_{\rm el}^{(1)} = -\frac{\vec{R}\times\vec{P}}{m_{\rm n}\,R^2}\,\langle\phi_{\rm el}|J_{\rm el}^j\,\frac{1}{(\mathcal{E}_{\rm el}-H_{\rm el})'}\,Q^j|\phi_{\rm el}\rangle, \tag{14}$$

where $\vec{J}_{\rm el}$ is the electronic angular momentum operator, and $1/m_{\rm n} = 1/m_A + 1/m_B$, so that the total spin-rotation constant c_A can be inferred from

$$-c_A\,\vec{I}\cdot\vec{J} = -\frac{\vec{I}\cdot\vec{J}}{m_{\rm n}\,R^2}\,\langle\phi_{\rm el}|\vec{J}_{\rm el}\,\frac{1}{(\mathcal{E}_{\rm el}-H_{\rm el})'}\,\vec{Q}_1|\phi_{\rm el}\rangle + \langle\phi_{\rm el}|\vec{Q}_2|\phi_{\rm el}\rangle\times\vec{P}\cdot\vec{I}. \tag{15}$$

The expectation value of the first term in $\vec{Q}_2$ [Eq. (12)] can alternatively be expressed in terms of a derivative of the BO energy, namely,

$$\langle\phi_{\rm el}|\sum_b\frac{e_A\,e}{4\pi}\,\frac{\vec{x}_b}{x_b^3}|\phi_{\rm el}\rangle = \vec{n}\left(\frac{\partial\mathcal{E}_{\rm el}}{\partial R} + \frac{e_A\,e_B}{4\pi}\,\frac{1}{R^2}\right), \tag{16}$$

and c_A in atomic units [$e_X = -Z_X\, e$, $\alpha = e^2/(4\,\pi)$] becomes

$$c_A = \alpha^2\left[\frac{1}{R^2}\,\frac{Z_A\, g_A}{2\, m_{\rm n}\, m_A}\,\langle\phi_{\rm el}|\sum_a \vec{x}_a\times\vec{p}_a\,\frac{1}{(\mathcal{E}_{\rm el}-H_{\rm el})}\sum_b\frac{\vec{x}_b\times\vec{p}_b}{x_b^3}|\phi_{\rm el}\rangle + \frac{1}{R}\,\frac{1}{2\, m_A^2}\,\frac{\partial\mathcal{E}_{\rm el}}{\partial R} + \frac{1}{R^3}\,\frac{Z_A\, Z_B\, g_A}{2\, m_{\rm n}\, m_A}\right]. \tag{17}$$

In the particular case of the proton and the deuteron in the HD molecule, we arrive at

$$c_p = \frac{\alpha^2}{2\,R^2\, m_{\rm n}\, m_p}\left[g_p\,\langle\phi_{\rm el}|\sum_a \vec{x}_a\times\vec{p}_a\,\frac{1}{(\mathcal{E}_{\rm el}-H_{\rm el})}\sum_b\frac{\vec{x}_b\times\vec{p}_b}{x_b^3}|\phi_{\rm el}\rangle + \frac{g_p}{R} + \frac{m_{\rm n}}{m_p}\,R\,\frac{\partial\mathcal{E}_{\rm el}}{\partial R}\right], \tag{18}$$

$$c_d = \frac{\alpha^2}{2\,R^2\, m_{\rm n}\, m_d}\left[g_d\,\langle\phi_{\rm el}|\sum_a \vec{x}_a\times\vec{p}_a\,\frac{1}{(\mathcal{E}_{\rm el}-H_{\rm el})}\sum_b\frac{\vec{x}_b\times\vec{p}_b}{x_b^3}|\phi_{\rm el}\rangle + \frac{g_d}{R} + \frac{m_{\rm n}}{m_d}\,R\,\frac{\partial\mathcal{E}_{\rm el}}{\partial R}\right], \tag{19}$$

where the sum goes over two electrons in the HD molecule. These formulas coincide with those derived originally in Ref. [13].

III. SPIN-SPIN CONSTANT d_1

The nuclear spin-spin direct interaction comes from the third term in Eq. (3) and is of the form

$$\delta H = \frac{e_A\, e_B}{4\,\pi}\,\frac{g_A\, g_B}{4\, m_A\, m_B}\,\frac{I_A^i\, I_B^j}{R^3}\left(\delta^{ij} - 3\,\frac{R^i\, R^j}{R^2}\right). \tag{20}$$

Using the fact that for the Σ states of a diatomic molecule $\vec{n}\cdot\vec{J}|J, M_J\rangle = 0$, the matrix elements of the angular part (in parentheses) in states with definite angular momentum J can be expressed in terms of this J as

$$\begin{aligned}&\langle J, M_J|\delta^{ij} - 3\,\frac{R^i\, R^j}{R^2}|J, M_J'\rangle\\ &\quad= \langle J, M_J|\frac{3\, J^i\, J^j + 3\, J^j\, J^i - 2\,\delta^{ij}\,\vec{J}^2}{(2\,J-1)\,(2\,J+3)}|J, M_J'\rangle.\end{aligned} \tag{21}$$

So, for such states, this interaction takes the form (in atomic units)

$$\begin{aligned}\delta H = \alpha^2\,&\frac{g_p\, g_d\, m_e^2}{4\, m_p\, m_d}\,\frac{1}{R^3}\\ &\times\,\frac{3\,(\vec{I}_p\cdot\vec{J})\,(\vec{I}_d\cdot\vec{J}) + 3\,(\vec{I}_d\cdot\vec{J})\,(\vec{I}_p\cdot\vec{J}) - 2\,(\vec{I}_p\cdot\vec{I}_d)\,\vec{J}^2}{(2\,J-1)\,(2\,J+3)}\end{aligned} \tag{22}$$

and the d_1 constant is

$$d_1 = \alpha^2\,\frac{g_p\, g_d\, m_e^2}{10\, m_p\, m_d}\,\frac{1}{R^3}. \tag{23}$$

IV. QUADRUPOLE CONSTANT d_2

The interaction of a particle possessing the electric quadrupole moment with the gradient of the electric field is given by

$$\delta H = -\,\frac{e}{6}\,Q^{ij}\,\partial_j E^i. \tag{24}$$

For a particle with a definite spin $I \geqslant 1$, the Q^{ij}, as a traceless and symmetric tensor, can be expressed in terms of a single scalar electric quadrupole moment Q defined by

$$Q^{ij} = \frac{Q}{I\,(2I-1)}\left(\frac{3}{2}\,I^i\, I^j + \frac{3}{2}I^j\, I^i - \delta^{ij}\,\vec{I}^2\right). \tag{25}$$

This definition is such that Q corresponds to the expectation value of Q^{33} in a state with the maximum value of M_I, namely,

$$Q = \langle I, I|Q^{33}|I, I\rangle. \tag{26}$$

The electric field is produced by the other nucleus and all the electrons. Let us introduce q, which is an averaged value of the gradient of the molecular electric field:

$$\begin{aligned}q &\equiv \frac{1}{3}\,\langle\phi_{\rm el}|e\,\partial_j E^i|\phi_{\rm el}\rangle\left(\delta^{ij} - 3\,\frac{R^i\, R^j}{R^2}\right)\\ &= \langle\phi_{\rm el}|\frac{\partial^2 V}{\partial R_d^i\,\partial R_d^j}\left(\frac{R^i\, R^j}{R^2} - \frac{\delta^{ij}}{3}\right)|\phi_{\rm el}\rangle,\end{aligned} \tag{27}$$

where V is the Coulomb interaction potential. Then, the traceless part of the electric-field gradient is

$$\langle\phi_{\rm el}|e\,\partial_j E^i|\phi_{\rm el}\rangle = \frac{q}{2}\left(\delta^{ij} - 3\,\frac{R^i\, R^j}{R^2}\right) \tag{28}$$

and in a state with the definite angular momentum

$$\begin{aligned}&\langle J, M_J, \phi_{\rm el}|e\,\partial_j E^i|\phi_{\rm el}, J, M_J'\rangle\\ &\quad= \frac{q}{2}\,\langle J, M_J|\frac{3\, J^i\, J^j + 3\, J^j\, J^i - 2\,\delta^{ij}\,\vec{J}^2}{(2\,J-1)\,(2\,J+3)}|J, M_J'\rangle.\end{aligned} \tag{29}$$

Finally, the interaction of the electric quadrupole moment of the nucleus with the gradient of the molecular electric field is

$$\begin{aligned}\delta H &= -\frac{1}{6}\,\frac{Q}{I\,(2I-1)}\left(\frac{3}{2}\,I^i\, I^j + \frac{3}{2}I^j\, I^i - \delta^{ij}\,\vec{I}^2\right)\\ &\quad\times\,\frac{q}{2}\,\frac{3\, J^i\, J^j + 3\, J^j\, J^i - 2\,\delta^{ij}\,\vec{J}^2}{(2\,J-1)\,(2\,J+3)}\\ &= -Q\,q\,\frac{3\,(\vec{I}\cdot\vec{J})^2 + \frac{3}{2}\,(\vec{I}\cdot\vec{J}) - \vec{I}^2\,\vec{J}^2}{2\,I\,(2I-1)\,(2\,J-1)\,(2\,J+3)}.\end{aligned} \tag{30}$$

The Ramsey constant d_2 is thus

$$d_2 = -\frac{Q\,q}{10}, \tag{31}$$

which in atomic units reads

$$d_2 = -\alpha^2\,\frac{Q}{10\lambda\!\!\!^{-2}}\,\langle\phi_{\rm el}|\frac{\partial^2 V}{\partial R_d^i\,\partial R_d^j}\left(\frac{R^i\, R^j}{R^2} - \frac{\delta^{ij}}{3}\right)|\phi_{\rm el}\rangle, \tag{32}$$

where $\lambda\!\!\!^{-}$ is the reduced Compton wavelength of an electron.

V. NUMERICAL CALCULATIONS OF HYPERFINE CURVES

To evaluate the electronic matrix elements present in c_p and c_d [see Eqs. (18) and (19)] we use explicitly correlated Gaussian (ECG) basis functions of Σ^+,

$$\phi_\Sigma = e^{-a_{1A}\, r_{1A}^2 - a_{1B}\, r_{1B}^2 - a_{2A}\, r_{2A}^2 - a_{2B}\, r_{2B}^2 - a_{12}\, r_{12}^2}, \tag{33}$$

and Π symmetry:

$$\phi_\Pi^i = (\vec{R}\times\vec{r}_1)^i\,\phi = \epsilon^{ijk} R^j r_1^k\,\phi_\Sigma. \tag{34}$$

We employed 256 basis functions of Eq. (33) to represent the electronic wave function $\phi_{\rm el}$. The same number of functions of Eq. (34) was used to form the internal basis set of the resolvent $1/(\mathcal{E}_{\rm el}-H_{\rm el})$. Their nonlinear parameters were determined variationally in a global optimization process independently at 44 internuclear distances. While the parameters of the $\phi_{\rm el}$ were determined by minimizing the electronic energy, the nonlinear parameters of the internal basis were optimized with respect to the functional

$$\langle\phi_{\rm el}|\sum_a \vec{x}_a\times\vec{p}_a\,\frac{1}{\mathcal{E}_{\rm el}-H_{\rm el}}\sum_b \vec{x}_b\times\vec{p}_b|\phi_{\rm el}\rangle. \tag{35}$$

Thanks to the optimization of the ϕ_Σ and ϕ_Π functions the relative numerical accuracy ($\approx 10^{-5}$) of the spin-rotation parameters is higher than the estimate of nonadiabatic corrections, and the use of only 256 basis functions was sufficient for this purpose. Apart from the second-order matrix element, the spin-rotation parameters c_p and c_d require evaluation of the derivative of the BO energy with respect to the intermolecular distance [see Eqs. (18) and (19)]. This derivative can be found from the virial theorem

$$\frac{\partial\mathcal{E}_{\rm el}}{\partial R} = \frac{\langle V\rangle_{\rm el} - 2\,\mathcal{E}_{\rm el}}{R}, \tag{36}$$

which enables calculations with high numerical precision.

The direct spin-spin interaction constant d_1 does not require evaluation of any electronic matrix elements and, for a given R, is fully determined by the well-known nuclear g factors and the electron-nucleus mass ratios.

Considering the matrix element of the quadrupole constant d_2 in Eq. (32), we integrated it by parts to obtain a less singular form,

$$\begin{aligned}\left\langle \frac{\partial^2 V}{\partial R_d^i\,\partial R_d^j}\left(\frac{R^iR^j}{R^2}-\frac{\delta^{ij}}{3}\right)\right\rangle &= \frac{2}{R^3} - \left(\frac{R^iR^j}{R^2}-\frac{\delta^{ij}}{3}\right)\\ &\times\int d^3r_1\,d^3r_2\left(\frac{1}{r_{1A}}\frac{\partial^2(\phi_{\rm el}^2)}{\partial r_1^i\,\partial r_1^j}+\frac{1}{r_{2A}}\frac{\partial^2(\phi_{\rm el}^2)}{\partial r_2^i\,\partial r_2^j}\right),\end{aligned} \tag{37}$$

which is more convenient in calculations. The above expectation value was evaluated with $\phi_{\rm el}$ expanded in an ECG basis as large as 1024 terms, due to slow numerical convergence. Table I supplies data which enable an analysis of this convergence at different regions of the internuclear distance. This analysis reveals that, depending on the region, four to six significant digits are stable. Our numerical results are in good agreement with the results published by Pavanello *et al.* [14] except for the shortest internuclear distances, at which their values seem to be less accurate. As a final result we take values from the 1024-term basis and note that the achieved numerical accuracy of the electric-field gradient within the BO approximation is higher than the estimated contribution from the nonadiabatic effects.

TABLE I. Convergence of the electric-field gradient q defined in Eq. (27) with the growing basis set size K at selected internuclear distances R in comparison with the most accurate literature data (all data in atomic units).

K	$R=0.4$	$R=1.4$	$R=5.0$
128	30.082378	0.338173	−0.001890827
256	30.082224	0.338084	−0.001887565
512	30.082195	0.338078	−0.001888152
1024	30.082184	0.338073	−0.001890408
[14][a]	30.405155	0.338070	−0.00189088
[15][b]		0.33630	

[a]Pavanello *et al.* [14].
[b]Reid and Vaida [15].

In contrast to previously described magnetic interactions, the electric quadrupole interaction constant d_2 depends on the electric quadrupole moment of the deuteron Q, which is not well known from independent measurements. In fact, it is the old Ramsey measurement [2], which allows the most accurate determination of the deuteron quadrupole moment. For this purpose we use the measurement for the $J=1$ level of the D_2 molecule, for which d_2 is found with the highest accuracy and the nonadiabatic effects are smaller in comparison to the HD molecule. This determination of Q is described in detail in the next section; however, we use this value here for evaluation of the d_2 curve. The final numerical results for the spin-rotation [c_p and c_d, Eqs. (18) and (19)], spin-spin [d_1, Eq. (23)], electric-field gradient [q, Eq. (27)], and quadrupole [d_2, Eq. (32)] constants for all the internuclear distances are presented in Table II. The conversion factor from energies in atomic units to frequencies in Hz is $2\,{\rm Ry}\,c$, where Ry is the Rydberg constant and c is the speed of light in a vacuum. For small R, all curves exhibit R^{-3} dependence as they should, while for large R they vanish faster than R^{-3}.

VI. HYPERFINE CONSTANTS

The data in Table II were interpolated at internuclear distances R between 0 and 5 bohrs, and extrapolated for $R>5$ bohrs by fitting $a_8/R^8+a_9/R^9+a_{10}/R^{10}+a_{11}/R^{11}$. This particular choice of powers of R being in agreement with numerical data does not affect averaged results within five significant digits for the low-lying levels. The averaged values, according to Eq. (2), were evaluated with the nuclear wave function corresponding to a (v,J) rovibrational level. This function is a solution of the radial nuclear equation, with nuclear masses and with the highly accurate BO potential obtained in Ref. [16], using the descrete variable representation method [17,18]. Numerical results for selected low-lying states of HD are shown in Table III, while for an arbitrary rovibrational level they can be obtained from the

TABLE II. The hyperfine splitting parameters (in kHz) and electric-field gradient q (in a.u.) evaluated with ECG wave functions at different internuclear distances, R (in a.u.). According to Eq. (23), $d_1(R)\,R^3 = 49.7735$. The deuteron quadrupole moment used here is $Q = 0.2856(2)$ fm^2 [see Eq. (40)]. The relative numerical uncertainty of c_p and c_d is about 10^{-5}, while that of q and d_2 is below 10^{-4} with the exception of large distances, i.e., $R > 4$ a.u.

R	$c_p(R)\,R^3$	$c_d(R)\,R^3$	$q(R)\,R^3$	$d_2(R)\,R^3$
0.00	383.478	53.8392	2	−134.306
0.05	383.343	53.8227	1.99993	−134.206
0.10	382.562	53.7266	1.99910	−134.150
0.20	378.132	53.1835	1.99045	−133.570
0.30	370.082	52.2006	1.96675	−131.979
0.40	359.411	50.9042	1.92526	−129.195
0.50	347.140	49.4211	1.86651	−125.253
0.60	334.055	47.8480	1.79257	−120.291
0.80	307.471	44.6783	1.60929	−107.992
1.00	282.174	41.6944	1.39463	−93.5873
1.10	270.345	40.3096	1.28044	−85.9243
1.20	259.127	39.0020	1.16374	−78.0931
1.30	248.527	37.7708	1.04579	−70.1780
1.40	238.531	36.6121	0.927672	−62.2517
1.50	229.121	35.5221	0.810308	−54.3760
1.60	220.252	34.4935	0.694516	−46.6057
1.70	211.885	33.5194	0.581002	−38.9883
1.80	203.974	32.5925	0.470417	−31.5675
1.90	196.458	31.7028	0.363340	−24.3820
2.00	189.296	30.8435	0.260328	−17.4693
2.10	182.429	30.0052	0.161886	−10.8634
2.20	175.786	29.1768	0.0685114	−4.59747
2.30	169.328	28.3518	−0.0193471	1.29829
2.40	162.990	27.5199	−0.101231	6.79314
2.50	156.723	26.6735	−0.176737	11.8600
2.60	150.493	25.8071	−0.245492	16.4738
2.70	144.243	24.9121	−0.307151	20.6115
2.80	137.942	23.9843	−0.361458	24.2557
2.90	131.585	23.0232	−0.408220	27.3937
3.00	125.125	22.0226	−0.447320	30.0175
3.20	111.965	19.9190	−0.502678	33.7323
3.40	98.5935	17.7071	−0.528954	35.4956
3.60	85.2803	15.4469	−0.529418	35.5267
3.80	72.4156	13.2191	−0.509111	34.1640
4.00	60.3781	11.1023	−0.473173	31.7524
4.20	49.4911	9.16421	−0.428052	28.7245
4.40	39.9395	7.44650	−0.378058	25.3697
4.60	31.7964	5.96901	−0.328370	22.0354
4.80	25.0220	4.72985	−0.279521	18.7573
5.00	19.4962	3.71147	−0.236301	15.8570
5.20	15.0626	2.88852	−0.197415	13.2476
5.40	11.5579	2.23328	−0.163798	10.9917
5.60	8.81557	1.71698	−0.134138	9.00133
5.80	6.68912	1.31383	−0.110457	7.41224
6.00	5.05561	1.00182	−0.0894048	5.99953

updated version of the publicly available H2SPECTRE computer code [7].

Considering the quadrupole moment of the deuteron, it can be determined from the electric quadrupole coupling constant d_2, obtained from Ramsey measurements performed for HD in the J=1 level [1], and for D_2 in $J = 1$ and 2 levels [2] in the ground vibrational state. Among them, the most accurate is the value

$$d_2 = -22.5037(14)\,\text{kHz} \tag{38}$$

obtained from the measurement for the J=1 level of D_2, which was later refined in Ref. [15]. Our value for the gradient of the electric field for this level is

$$\langle q \rangle = 0.33535(18)\ \text{a.u.} \tag{39}$$

The quadrupole moment, obtained using this value and Eq. (32), is

$$Q = -\frac{d_2}{2\,Ry\,c}\,\frac{10\lambda\!\!\!^{-2}}{\alpha^2\,\langle q \rangle} = 0.2856(2)\,\text{fm}^2. \tag{40}$$

Its uncertainty comes from the neglected nonadiabatic effects, which are of the order of the ratio of the electron mass to the reduced nuclear mass $m_n(D_2)$. This quadrupole moment Q is used in Table II to obtain the electric quadrupole constant d_2 as a function of R and in Table III for various rovibrational levels.

A similar relative uncertainty of $1/m_n(\text{HD}) \approx 0.8 \times 10^{-3}$ due to the omitted nonadiabatic effects is assumed for all hyperfine constants in Tables III and IV. Because this uncertainty is larger than our numerical uncertainties, the latter were neglected. Moreover, we expect that theoretical predictions for d_2 shall be in fact more accurate due to partial cancellation between nonadiabatic effects in D_2 and HD. Indeed, in comparison to measurements performed by Quinn *et al.* [1] (see Table IV), all our values differ by about σ, with the exception of d_2, which differs by only $\sigma/3$. In conclusion, all our results are in agreement with experimental values.

Considering the comparison with previous theoretical calculations, our quadrupole moment of the deuteron $Q = 0.2856(2)$ fm^2 differs within uncertainties from values obtained by Pavanello *et al.* [14], 0.285 783(30) fm^2; Bishop and Cheung [19], 0.2862(15) fm^2; and Reid and Vaida [20,21], 0.2860(15) fm^2. Surprisingly, the result of Ref. [14] has tighter error bars than that of our paper, most probably due to underestimation of nonadiabatic effects.

Results of the hyperfine parameters for the HD molecule, but without any uncertainties, have been obtained by Dupré [6], who considered three vibrational levels ($v = 0,\ 1,\ 2$) with the rotational quantum number $J = 1$. His results are presented in Table IV after conversion from a different notation ($d_1 = 2\,c_{\text{dip}}/5$, $d_2 = -c_{\text{quad}}/10$). As one can notice, his results for the $v = 0$, $J = 1$ level differ from the experimental ones by several hundreds of Hz. A similar difference appears in comparison with our values and this difference grows with the vibrational quantum number. Moreover, very recent work [22] by the Toruń group presents results for hyperfine parameters for all molecular levels of HD (in the ground electronic state), but again without any uncertainties. Differences for d_1 and d_2 parameters are very small and, most probably, come from a different radial equation for the nuclear wave function χ, while differences for c_p and c_d parameters are larger, but at any rate they are in better agreement with our results.

TABLE III. Theoretically predicted hyperfine splitting parameters and levels (in kHz) for a selection of the lowest rovibrational levels (v, J). The energy shifts $\delta E_F^{\pm}$ are labeled with the total angular momentum F and with $\pm$, which distinguishes between hyperfine levels of the same F but different energy.

(v, J)	$\langle c_p \rangle$	$\langle c_d \rangle$	$\langle d_1 \rangle$	$\langle d_2 \rangle$	$\delta E_{J+\frac{3}{2}}$	$\delta E^{-}_{J+\frac{1}{2}}$	$\delta E^{+}_{J+\frac{1}{2}}$	$\delta E^{-}_{J-\frac{1}{2}}$	$\delta E^{+}_{J-\frac{1}{2}}$	$\delta E_{J-\frac{3}{2}}$
(0,1)	85.675	13.132	17.773	−22.459	−58.3	−1.9	54.1	−117.0	187.5	
(0,2)	84.970	13.028	17.650	−22.212	−114.3	−30.1	67.7	−115.2	209.8	155.1
(0,3)	83.930	12.874	17.468	−21.850	−168.2	−67.3	90.8	−135.9	244.4	210.6
(0,4)	82.573	12.674	17.231	−21.377	−219.6	−105.6	115.5	−159.0	279.2	262.4
(1,1)	84.067	12.846	17.225	−22.305	−57.4	−1.6	53.8	−115.8	183.7	
(1,2)	83.356	12.742	17.102	−22.057	−112.4	−29.0	66.8	−113.5	206.2	150.9
(1,3)	82.308	12.588	16.922	−21.691	−165.2	−65.4	89.3	−133.6	240.1	205.4
(1,4)	80.942	12.387	16.686	−21.216	−215.6	−102.9	113.4	−156.2	274.2	256.2
(2,1)	82.183	12.524	16.654	−22.043	−56.3	−1.4	53.3	−114.1	179.3	
(2,2)	81.470	12.420	16.533	−21.794	−110.1	−27.8	65.5	−111.4	201.8	146.3
(2,3)	80.418	12.265	16.354	−21.427	−161.6	−63.3	87.5	−130.9	235.0	199.8
(2,4)	79.048	12.064	16.120	−20.950	−210.7	−99.9	111.0	−152.9	268.3	249.3

VII. HYPERFINE STRUCTURE AND INDIVIDUAL TRANSITION RATES

The hyperfine structure for each molecular level (v, J) is obtained by diagonalization of the Hamiltonian $H_{\rm hfs}(v, J)$ in Eq. (1). We perform this diagonalization in the basis of $|J, M_J; I_p, M_p; I_d, M_d\rangle$ states because this basis is convenient for the later calculation of transition rates. Explicit formulas for eigenvalues δE_F (F is the total angular momentum) for $J = 1, \ldots, 4$ are given in the Appendix, while their numerical values are presented in Table III. These eigenvalues represent the shift of the molecular hyperfine level with respect to the centroid. These hyperfine levels extend in the range of several hundreds of kHz, e.g., 300 kHz for the (2,1) state and 500 kHz for the (0,4) state, and they are still much smaller than the discrepancy of the order of 1 MHz between Hefei [5] and Amsterdam measurement [4] of the overtone $R(1)$ line in HD, which remains to be explained. Uncertainties in our hyperfine levels mainly come from the neglected nonadiabatic effects and this is already included in the hyperfine coefficient. However, we do not perform detailed analysis of the resulting uncertainty of individual hyperfine levels, but in general it should be about 0.1 kHz, if not less.

TABLE IV. Comparison of our theoretically predicted hyperfine splitting parameters (in kHz) with the available experimental [1] and theoretical [6] literature data.

(v, J)	$\langle c_p \rangle$	$\langle c_d \rangle$	$\langle d_1 \rangle$	$\langle d_2 \rangle$
(0,1)	85.675(60)	13.132(9)	17.773(12)	−22.459(16)
Exper.[a]	85.600(18)	13.122(11)	17.761(12)	−22.454(6)
Theory[b]	86.2832	13.2450	17.8317	−22.66493
Theory[c]	85.84	13.18	17.758	−22.4540
(1,1)	84.067(60)	12.846(9)	17.225(12)	−22.305(16)
Theory[b]	85.0775	13.0599	17.2842	−22.50968
Theory[c]	84.63	12.99	17.211	−22.3018
(2,1)	82.183(60)	12.524(9)	16.654(12)	−22.043(16)
Theory[b]	83.5670	12.8280	16.7190	−22.25516
Theory[b]	83.09	12.75	16.642	−22.0415

[a]Quinn *et al.* [1].
[b]Dupré [6].
[c]Jóźwiak *et al.* [22].

Regarding hyperfine resolved transition rates, the main factor determining the line intensity is the square of the transition electric dipole moment. Because we are interested here in relative intensities, we consider only its angular part, which is

$$|\vec{d}_{if}|^2 = \sum_{M_i} \sum_{M_f} |\langle F_f, M_f|\vec{n}|F_i, M_i\rangle|^2, \tag{41}$$

where the double sum goes over all the possible projections of the total angular momenta of both the final and initial state. The above matrix elements were evaluated with the eigenfunctions of the $H_{\rm hfs}(v, J)$ in the previously mentioned basis of $|J, M_J; I_p, M_p; I_d, M_d\rangle$ functions.

We now turn to analysis of recent measurements. There are several very accurate measurements reported in literature concerning the infrared absorption in HD. All of them have uncertainties much below 100 kHz assigned to the transition energy. We have determined the hyperfine splittings for the initial and final states involved in these transitions and estimated the relative intensities for all the hyperfine components. The obtained stick spectra were dressed with the Lorentzian line shapes in order to simulate the overall line shape.

A. $R_2(1)$ transition

The first transition line of interest is the $R_2(1)$ or $(0, 1) \rightarrow (2, 2)$ line. This transition was studied by three different experimental groups reporting the following transition energies: Fasci *et al.* [3], 217 105 181.581(94) MHz; Cozijn *et al.* [4], 217 105 181.895(20) MHz; and Tao *et al.* [5], 217 105 182.79(3)(8) MHz. The disagreement between these results can, at least partially, be attributed to the unresolved hyperfine structure of the line. A thorough analysis of the pressure-dependent line shapes related to the hyperfine splitting of the involved rovibrational levels has been performed in Ref. [23] and resulted in a refined transition frequency for this line equal to 217 105 181.901(50) MHz. The corresponding theoretical prediction for this transition is

TABLE V. Theoretically predicted line list of the hyperfine splitting of the $R_2(1)$ line. F is the total angular momentum quantum number. The label + or − distinguishes levels of the same F but different energy (see Table III).

$\|F_i\rangle \rightarrow \|F_f\rangle$	δE (kHz)	$\|\vec{d}_{if}\|^2$
$\|\frac{1}{2}+\rangle \rightarrow \|\frac{3}{2}-\rangle$	−298.9	0.042
$\|\frac{3}{2}+\rangle \rightarrow \|\frac{3}{2}-\rangle$	−165.5	0.101
$\|\frac{3}{2}-\rangle \rightarrow \|\frac{3}{2}-\rangle$	−109.5	0.344
$\|\frac{3}{2}+\rangle \rightarrow \|\frac{5}{2}-\rangle$	−82.0	0.116
$\|\frac{5}{2}\rangle \rightarrow \|\frac{3}{2}-\rangle$	−53.1	0.024
$\|\frac{5}{2}\rangle \rightarrow \|\frac{7}{2}\rangle$	−51.8	3.200
$\|\frac{1}{2}+\rangle \rightarrow \|\frac{1}{2}\rangle$	−41.2	0.435
$\|\frac{3}{2}-\rangle \rightarrow \|\frac{5}{2}-\rangle$	−25.9	1.987
$\|\frac{1}{2}-\rangle \rightarrow \|\frac{3}{2}-\rangle$	5.6	1.089
$\|\frac{3}{2}+\rangle \rightarrow \|\frac{5}{2}+\rangle$	11.4	1.659
$\|\frac{1}{2}+\rangle \rightarrow \|\frac{3}{2}+\rangle$	14.3	0.857
$\|\frac{5}{2}\rangle \rightarrow \|\frac{5}{2}-\rangle$	30.5	0.296
$\|\frac{3}{2}-\rangle \rightarrow \|\frac{5}{2}+\rangle$	67.5	0.317
$\|\frac{3}{2}+\rangle \rightarrow \|\frac{1}{2}\rangle$	92.2	0.116
$\|\frac{5}{2}\rangle \rightarrow \|\frac{5}{2}+\rangle$	123.9	0.424
$\|\frac{3}{2}+\rangle \rightarrow \|\frac{3}{2}+\rangle$	147.7	0.674
$\|\frac{3}{2}-\rangle \rightarrow \|\frac{1}{2}\rangle$	148.2	0.018
$\|\frac{3}{2}-\rangle \rightarrow \|\frac{3}{2}+\rangle$	203.7	0.000
$\|\frac{5}{2}\rangle \rightarrow \|\frac{3}{2}+\rangle$	260.1	0.056
$\|\frac{1}{2}-\rangle \rightarrow \|\frac{1}{2}\rangle$	263.3	0.232
$\|\frac{1}{2}-\rangle \rightarrow \|\frac{3}{2}+\rangle$	318.8	0.013

217 105 180.2(0.9) MHz [24]. Table V and Fig. 1 present the theoretical hyperfine spectrum for this absorption line.

B. $P_2(1)$ transition

Diouf *et al.* [25] measured the $P_2(1)$ or $(0,1) \rightarrow (2,0)$ absorption line and, employing the line-shape analysis mentioned above, obtained the transition frequency 209 784 242 007(20) kHz. The uncertainty of 20 kHz is more than an order of magnitude smaller than the extent of the hyperfine splitting (≈300 kHz). The calculated frequency for this transition line is 209 784 240.1(1.0) MHz [7,26]. The theoretical model of the hyperfine spectrum is shown in Table VI and Fig. 2.

TABLE VI. Theoretically predicted line list of the hyperfine splitting of the $P_2(1)$ line. F is the total angular momentum quantum number. The label + or − distinguishes levels of the same F but different energy (see Table III).

$\|F_i\rangle \rightarrow \|F_f\rangle$	δE (kHz)	$\|\vec{d}_{if}\|^2$
$\|\frac{1}{2}+\rangle \rightarrow \|\frac{1}{2}-\rangle$	−187.5	0.232
$\|\frac{1}{2}+\rangle \rightarrow \|\frac{3}{2}\rangle$	−187.5	0.435
$\|\frac{3}{2}+\rangle \rightarrow \|\frac{1}{2}-\rangle$	−54.1	0.177
$\|\frac{3}{2}+\rangle \rightarrow \|\frac{3}{2}\rangle$	−54.1	1.156
$\|\frac{3}{2}-\rangle \rightarrow \|\frac{3}{2}\rangle$	1.9	0.177
$\|\frac{3}{2}-\rangle \rightarrow \|\frac{1}{2}-\rangle$	1.9	1.156
$\|\frac{5}{2}\rangle \rightarrow \|\frac{3}{2}\rangle$	58.3	2.000
$\|\frac{1}{2}-\rangle \rightarrow \|\frac{3}{2}\rangle$	117.0	0.232
$\|\frac{1}{2}-\rangle \rightarrow \|\frac{1}{2}-\rangle$	117.0	0.435

C. $R_1(0)$ transition

Fast and Meek [27] recently measured the $R_1(0)$, i.e., $(0,0) \rightarrow (1,1)$, transition using double resonance spectroscopy in a molecular beam. The transition frequency of 111 448 815 477(13) kHz was determined with unprecedented relative accuracy of 1.2×10^{-10}. The absolute uncertainty of 13 kHz is over 20 times smaller than the 300-kHz extent of hyperfine splitting in the upper rovibrational level. This experimental result can be compared with the theoretically predicted frequency of 111 448 814.5(6) MHz [7,26]. A theoretical absorption spectrum pertinent to this transition is shown in Table VII and Fig. 3.

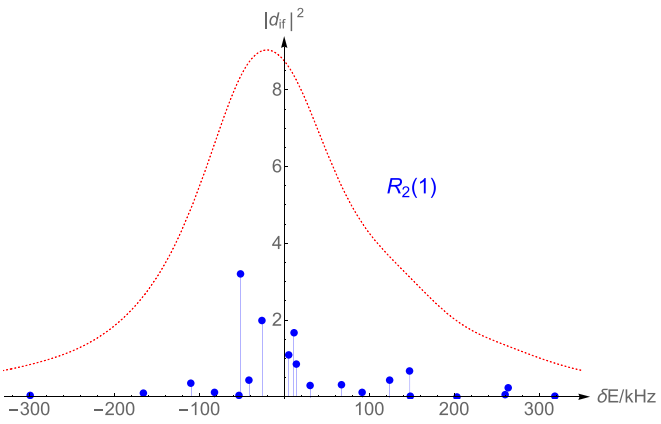

FIG. 1. Graphical representation of the $R_2(1)$ line. The dotted line represents a Lorentzian line shape with FWHM = 150 kHz, superimposed on the stick spectrum.

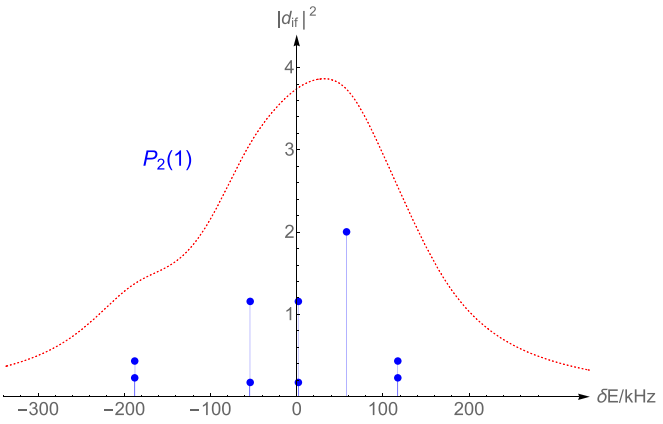

FIG. 2. Graphical representation of the $P_2(1)$ line. The dotted line represents a Lorentzian line shape with FWHM = 150 kHz, superimposed on the stick spectrum.

TABLE VII. Theoretically predicted line list of the hyperfine splitting of the $R_1(0)$ line. F is the total angular momentum quantum number. The label + or − distinguishes levels of the same F but different energy (see Table III).

$\|F_i\rangle \rightarrow \|F_f\rangle$	δE(kHz)	$\|\vec{d}_{if}\|^2$
$\|\frac{3}{2}\rangle \rightarrow \|\frac{1}{2}-\rangle$	−115.8	0.234
$\|\frac{1}{2}-\rangle \rightarrow \|\frac{1}{2}-\rangle$	−115.8	0.433
$\|\frac{3}{2}\rangle \rightarrow \|\frac{5}{2}\rangle$	−57.4	2.000
$\|\frac{3}{2}\rangle \rightarrow \|\frac{3}{2}-\rangle$	−1.6	0.170
$\|\frac{1}{2}-\rangle \rightarrow \|\frac{3}{2}-\rangle$	−1.6	1.163
$\|\frac{1}{2}-\rangle \rightarrow \|\frac{3}{2}+\rangle$	53.8	0.170
$\|\frac{3}{2}\rangle \rightarrow \|\frac{3}{2}+\rangle$	53.8	1.163
$\|\frac{1}{2}-\rangle \rightarrow \|\frac{1}{2}+\rangle$	183.7	0.234
$\|\frac{3}{2}\rangle \rightarrow \|\frac{1}{2}+\rangle$	183.7	0.433

VIII. SUMMARY AND OUTLOOK

We performed the derivation and the numerical calculation of the leading hyperfine interactions in the HD molecule. Moreover, we obtained hyperfine constants for all low-lying levels of HD and compared with experimental and previous theoretical results. The accuracy of our calculations is limited by the unknown nonadiabatic effects, which are estimated by the ratio of the electron mass to the reduced nuclear mass. Very good agreement is achieved with results of the measurements by Quinn *et al.* [1] for the first rotational state of HD. From the measurement of the d_2 constant in the D_2 molecule [2,15] we determined the value of the deuteron quadrupole moment in agreement with the previous determinations, but with greater accuracy. However, our results for the hyperfine constants in HD differ from the previous calculations in Ref. [6] by hundreds of Hz for $v = 0$ and this difference grows with the vibrational number.

All the nonadiabatic effects, which presently limit our accuracy, can be calculated with the use of a very accurate nonadiabatic wave function expanded in explicitly correlated exponential [28] basis. This requires, however, the development of integrals with quadratic inverse powers of interparticle distances, and we are presently pursuing this project.

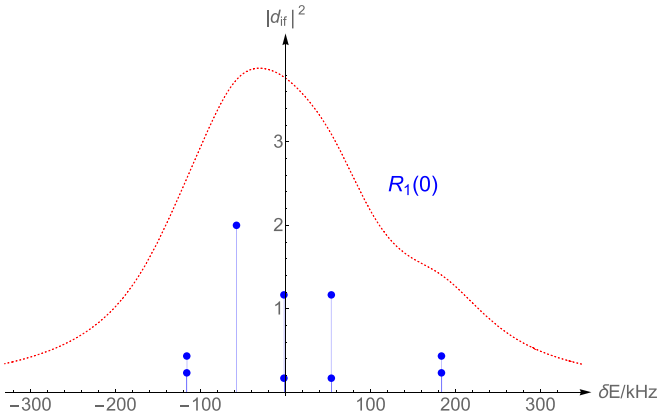

FIG. 3. Graphical representation of the $R_1(0)$ line. The dotted line represents a Lorentzian line shape with FWHM = 150 kHz, superimposed on the stick spectrum.

Although we did not calculate relativistic corrections to the hyperfine coefficients, we stress their importance in achieving high-precision theoretical predictions for the molecular hfs. They are of particular interest for an improved determination of the deuteron quadrupole moment. These relativistic corrections can be calculated in the BO approximation, as previously done for the nuclear spin-spin coupling [29]. To perform such calculations, however, appropriate formulas have to be derived. Ramsey, in 1953 [30], worked out formulas for the nuclear spin-spin interactions. In a similar way, one can obtain relativistic corrections to the electric quadrupole moment and to the spin-rotation constants. Having a pertinent theoretical framework, one can calculate all these hyperfine constants with a relative accuracy of α^3/π, limited by the unknown QED effects. Numerically it is about 10^{-7}, and we claim that this accuracy can be achieved for all the hyperfine parameters in HD, H_2, and D_2 molecules. Such accuracy will give an opportunity for high-precision tests of molecular hyperfine interactions, provided that measurements of similar accuracy are performed. We hope that the present paper will encourage experimentalists to undertake this challenge.

ACKNOWLEDGMENTS

This research was supported by National Science Center (Poland) Grant No. 2016/23/B/ST4/01821 as well as by a computing grant from Poznań Supercomputing and Networking Center and by PL-Grid Infrastructure.

APPENDIX: EIGENVALUES OF $H_{\rm hfs}$ FOR THE LOWEST J

In this section analytic formulas for the eigenvalues of the hyperfine Hamiltonian are provided. The labeling of the eigenvalues δE corresponds to that used in Table III. For simplicity, the symbol of the rovibrational averaging was dropped here, i.e., $c_p \equiv \langle c_p \rangle$, etc.

1. $J = 1$

$$\delta E_{5/2} = -c_d - \frac{c_p}{2} + \frac{d_1}{2} + \frac{d_2}{2}, \tag{A1}$$

$$\delta E^{\pm}_{3/2} = \frac{c_p}{4} - d_1 - d_2 \pm \frac{1}{4}\sqrt{A_1}, \tag{A2}$$

$$\delta E^{\pm}_{1/2} = \frac{3c_d}{2} + \frac{c_p}{4} + \frac{5d_1}{4} + \frac{5d_2}{4} \pm \frac{1}{4}\sqrt{B_1}, \tag{A3}$$

$$A_1 = -16c_dc_p - 16d_1c_p + 24d_2c_p + 16c_d^2 - 8d_1c_d - 48d_2c_d + 9c_p^2 + 21d_1^2 + 36d_2^2 + 12d_1d_2, \tag{A4}$$

$$B_1 = -4c_dc_p + 50d_1c_p - 30d_2c_p + 4c_d^2 - 20d_1c_d + 60d_2c_d + 9c_p^2 + 75d_1^2 + 225d_2^2 - 150d_1d_2. \tag{A5}$$

2. $J = 2$

$$\delta E_{7/2} = -2c_d - c_p + \frac{5d_1}{7} + \frac{5d_2}{7}, \tag{A6}$$

$$\delta E^{\pm}_{5/2} = -\frac{c_d}{2} + \frac{c_p}{4} - \frac{25d_1}{28} - \frac{25d_2}{28} \pm \frac{1}{28}\sqrt{B_2}, \tag{A7}$$

$$\delta E^{\pm}_{3/2} = 2c_d + \frac{c_p}{4} \pm \frac{1}{4}\sqrt{A_2}, \tag{A8}$$

$$\delta E_{1/2} = 3c_d + \frac{3c_p}{2} + \frac{5d_1}{2} + \frac{5d_2}{2}, \tag{A9}$$

$$\begin{aligned} A_2 = {} & -32c_dc_p + 40d_1c_p - 80d_2c_p + 16c_d^2 \\ & - 40d_1c_d + 80d_2c_d + 25c_p^2 + 25d_1^2 \\ & + 100d_2^2 - 100d_1d_2, \end{aligned} \tag{A10}$$

$$\begin{aligned} B_2 = {} & -2548c_dc_p - 1190d_1c_p + 2730d_2c_p \\ & + 1764c_d^2 + 140d_1c_d - 3780d_2c_d + 1225c_p^2 \\ & + 975d_1^2 + 2025d_2^2 - 150d_1d_2. \end{aligned} \tag{A11}$$

3. $J = 3$

$$\delta E_{9/2} = -3c_d - \frac{3c_p}{2} + \frac{5d_1}{6} + \frac{5d_2}{6}, \tag{A12}$$

$$\delta E^{\pm}_{7/2} = -c_d + \frac{c_p}{4} - \frac{5d_1}{6} - \frac{5d_2}{6} \pm \frac{1}{12}\sqrt{B_3}, \tag{A13}$$

$$\delta E^{\pm}_{5/2} = \frac{5c_d}{2} + \frac{c_p}{4} - \frac{d_1}{4} - \frac{d_2}{4} \pm \frac{1}{4}\sqrt{A_3}, \tag{A14}$$

$$\delta E_{3/2} = 4c_d + 2c_p + 2d_1 + 2d_2, \tag{A15}$$

$$\begin{aligned} A_3 = {} & -76c_dc_p + 46d_1c_p - 114d_2c_p + 36c_d^2 \\ & - 52d_1c_d + 108d_2c_d + 49c_p^2 + 21d_1^2 \\ & + 81d_2^2 - 78d_1d_2, \end{aligned} \tag{A16}$$

$$\begin{aligned} B_3 = {} & -936c_dc_p - 300d_1c_p + 780d_2c_p + 576c_d^2 \\ & + 120d_1c_d - 960d_2c_d + 441c_p^2 + 175d_1^2 \\ & + 400d_2^2 - 100d_1d_2. \end{aligned} \tag{A17}$$

4. $J = 4$

$$\delta E_{11/2} = -4c_d - 2c_p + \frac{10d_1}{11} + \frac{10d_2}{11}, \tag{A18}$$

$$\delta E^{\pm}_{9/2} = -\frac{3c_d}{2} + \frac{c_p}{4} - \frac{35d_1}{44} - \frac{35d_2}{44} \pm \frac{1}{44}\sqrt{B_4}, \tag{A19}$$

$$\delta E^{\pm}_{7/2} = 3c_d + \frac{c_p}{4} - \frac{5d_1}{14} - \frac{5d_2}{14} \pm \frac{1}{28}\sqrt{A_4}, \tag{A20}$$

$$\delta E_{5/2} = 5c_d + \frac{5c_p}{2} + \frac{25d_1}{14} + \frac{25d_2}{14}, \tag{A21}$$

$$\begin{aligned} A_4 = {} & -6664c_dc_p + 2660d_1c_p - 7140d_2c_p \\ & + 3136c_d^2 - 3080d_1c_d + 6720d_2c_d \\ & + 3969c_p^2 + 975d_1^2 + 3600d_2^2 - 3300d_1d_2, \end{aligned} \tag{A22}$$

$$\begin{aligned} B_4 = {} & -20812c_dc_p - 5170d_1c_p + 14190d_2c_p \\ & + 12100c_d^2 + 2860d_1c_d - 16500d_2c_d \\ & + 9801c_p^2 + 2325d_1^2 + 5625d_2^2 - 1950d_1d_2. \end{aligned} \tag{A23}$$

[1] W. E. Quinn, J. M. Baker, J. T. LaTourrette, and N. F. Ramsey, Phys. Rev. **112**, 1929 (1958).
[2] R. F. Code and N. F. Ramsey, Phys. Rev. A **4**, 1945 (1971).
[3] E. Fasci, A. Castrillo, H. Dinesan, S. Gravina, L. Moretti, and L. Gianfrani, Phys. Rev. A **98**, 022516 (2018).
[4] F. M. J. Cozijn, P. Dupré, E. J. Salumbides, K. S. E. Eikema, and W. Ubachs, Phys. Rev. Lett. **120**, 153002 (2018).
[5] L.-G. Tao, A.-W. Liu, K. Pachucki, J. Komasa, Y. R. Sun, J. Wang, and S.-M. Hu, Phys. Rev. Lett. **120**, 153001 (2018).
[6] P. Dupré, Phys. Rev. A **101**, 022504 (2020).
[7] P. Czachorowski, H2SPECTRE version 7.3, Fortran source code, 2020, Ph.D. thesis, University of Warsaw, 2019, https://www.fuw.edu.pl/~krp/codes.html; http://qcg.home.amu.edu.pl/H2Spectre.html; this version includes hyperfine parameters for HD and HT.
[8] J. Brown and A. Carrington, *Rotational Spectroscopy of Diatomic Molecules* (Cambridge University, New York, 2003).
[9] N. F. Ramsey and H. R. Lewis, Phys. Rev. **108**, 1246 (1957).
[10] N. Ramsey, *Molecular Beams* (Oxford University, New York, 1956).
[11] K. Pachucki, Phys. Rev. A **81**, 032505 (2010).
[12] 2018 CODATA recommended values, 2018, https://physics.nist.gov/cuu/Constants.
[13] R. V. Reid and A. H.-M. Chu, Phys. Rev. A **9**, 609 (1974).
[14] M. Pavanello, W.-C. Tung, and L. Adamowicz, Phys. Rev. A **81**, 042526 (2010).
[15] R. V. Reid and M. L. Vaida, Phys. Rev. A **7**, 1841 (1973).
[16] K. Pachucki, Phys. Rev. A **82**, 032509 (2010).
[17] D. T. Colbert and W. H. Miller, J. Chem. Phys. **96**, 1982 (1992).
[18] G. C. Groenenboom and D. T. Colbert, J. Comp. Phys. **99**, 9681 (1993).
[19] D. M. Bishop and L. M. Cheung, Phys. Rev. A **20**, 381 (1979).
[20] R. V. Reid and M. L. Vaida, Phys. Rev. Lett. **29**, 494 (1972).
[21] R. V. Reid and M. L. Vaida, Phys. Rev. Lett. **34**, 1064 (1975).
[22] H. Jóźwiak, H. Cybulski, and P. Wcislo, J. Quant. Spectrosc. Radiat. Transf. **253**, 107171 (2020).
[23] M. L. Diouf, F. M. J. Cozijn, B. Darquié, E. J. Salumbides, and W. Ubachs, Opt. Lett. **44**, 4733 (2019).
[24] P. Czachorowski, M. Puchalski, J. Komasa, and K. Pachucki, Phys. Rev. A **98**, 052506 (2018).
[25] M. L. Diouf, F. M. J. Cozijn, K.-F. Lai, E. J. Salumbides, and W. Ubachs, Phys. Rev. Research **2**, 023209 (2020).
[26] J. Komasa, M. Puchalski, P. Czachorowski, G. Łach, and K. Pachucki, Phys. Rev. A **100**, 032519 (2019).
[27] A. Fast and S. A. Meek, Phys. Rev. Lett. **125**, 023001 (2020).
[28] K. Pachucki and J. Komasa, Phys. Chem. Chem. Phys. **20**, 26297 (2018).
[29] M. Puchalski, J. Komasa, and K. Pachucki, Phys. Rev. Lett. **120**, 083001 (2018).
[30] N. F. Ramsey, Phys. Rev. **91**, 303 (1953).